Journal of
Mechanics of
Materials and Structures

NUMERICAL AND EXPERIMENTAL STUDY ON INCREMENTAL FORMING PROCESS OF AL/CU BIMETALS: INFLUENCE OF PROCESS PARAMETERS ON THE FORMING FORCE, DIMENSIONAL ACCURACY AND THICKNESS VARIATIONS

Mohammad Honarpisheh, Morteza Keimasi and Iman Alinaghian

Volume 13, No. 1 January 2018

msp

JOURNAL OF MECHANICS OF MATERIALS AND STRUCTURES
Vol. 13, No. 1, 2018
dx.doi.org/10.2140/jomms.2018.13.35

NUMERICAL AND EXPERIMENTAL STUDY ON INCREMENTAL FORMING PROCESS OF AL/CU BIMETALS: INFLUENCE OF PROCESS PARAMETERS ON THE FORMING FORCE, DIMENSIONAL ACCURACY AND THICKNESS VARIATIONS

MOHAMMAD HONARPISHEH, MORTEZA KEIMASI AND IMAN ALINAGHIAN

In the present study, a finite element method was carried out on the single point incremental forming process of explosive-welded Al/Cu bimetal. The effect of process parameters, such as the tool diameter, vertical pitch, sheet thickness, pyramid angle, and process strategies, were investigated on the forming forces, dimensional accuracy, and thickness distribution of a truncated pyramid with FEM approaches. The results obtained from the simulation were validated by experiments. The findings indicated that by increasing the tool radius and vertical pitch size, the forming force increases and the wall thickness decreases. The finite element prediction for forming force, thickness distribution, and process strategies shown good agreement with experiments.

1. Introduction

Single point incremental forming (SPIF) is a manufacturing process whereby a metal sheet is locally deformed by series of incremental tool movements using predefined paths. The main components of a SPIF process are these: blank, blank holder, backing plate, and forming tool. This process requires a computerized forming machine such as a CNC milling machine to allow the forming tool to move along the desired path. The SPIF process is suitable for manufacturing sheet metal components for small class production or prototyping [Jeswiet et al. 2005; Mulay et al. 2017]. Manco and Ambrogio [2010] present the principal of SPIF. There are many studies on SPIF; among them is [Bao et al. 2015], where the authors investigated the formability and microstructure of AZ31B alloy in an electropulse-assisted incremental forming process. The tool diameter can highly affect failure during SPIF process; Silva et al. [2011] investigated it by forming the limit curve for a AA1050-H11 sheet. Hirt et al. [2004] presented various forming strategies to find the maximum possible wall angle and minimum geometric deviations. Reddy and Cao [2009] proposed two types of incremental forming in terms of positive and negative incremental forming, whereby negative incremental forming refers to SPIF and positive incremental forming refers to two point incremental forming. Martins et al. [2008] presented a theoretical model for tool radius to show the stress state in a SPIF process. Yamashita et al. [2008] showed that a spiral tool path provides a better wall thickness distribution. Obikawa et al. [2009] investigated the effect of a high tool rotational speed on the SPIF of aluminum foils. Thibaud et al. [2012] did a simulation on a SPIF process. They found that the forces obtained by FEM confirms measured values from experiments. Arfa et al. [2013] demonstrated the effect of process parameters on the forming forces, mechanical properties, and geometrical accuracy of SPIF parts. Petek et al. [2009] investigated the impact of the wall angle, tool rotational speed, tool step

Keywords: incremental sheet forming, force, dimensional accuracy, explosive welding, FEM.

alloy	chemical compositions (wt. %)						
	Cu	Mn	Si	Mg	Zn	Fe	Al
Al-1050	0.0292	0.0177	0.101	0.0169	0.0158	0.479	base
C-10100	99.99	< 0.0002	< 0.0004	< 0.0001	0.00042	0.0032	0.001

alloy	mechanical properties	
	hardness Vickers (Hv)	yield stress (MPa)
Al-1050	26.1	39.5
C-10100	54.3	137

Table 1. Chemical compositions and mechanical properties of Al-1050 and Copper (C-10100).

size, tool diameter, and lubrication on the forming force and plastic strain. Cui et al. [2013] used new mathematical models, such as hyperbolic cone, skew cone, and elliptical cone, to model and validate the deformation process of incremental sheet forming. Capece Minutolo et al. [2007] evaluated the maximum slope angle of simple geometries in the incremental forming process. They investigated the maximum slope angle of frustums of a pyramid and a cone. They used the FE code to have an instrument evaluate the limits of the process in regards to the geometry of the manufacturing product. Centeno et al. [2014] studied the critical analysis of necking and fracture limit strains and forming forces in single point incremental forming. Ambrogio et al. [2004] investigated the influence of the process parameters on the accuracy through a reliable statistical analysis. Honarpisheh et al. [2016a] studied experimentally and numerically of the hot incremental forming of a Ti-6Al-4V sheet using electrical current.

Explosive-welded materials are new materials which are used in different sectors, such as aerospace and food industries. Many researches have been done on the explosive welding process. Performing the postprocess on the explosive-welded multilayers is an attractive field for new researches. The effect of cold rolling [Honarpisheh et al. 2016b; Asemabadi et al. 2012] and heat treatment [Akbari Mousavi and Sartangi 2008; Honarpisheh et al. 2012] have been performed on the explosive-welded multilayers. Al/Cu multilayers are one of the materials which are investigated in some researches [Ashani and Bagheri 2009; Gulenc 2008; Sedighi and Honarpisheh 2012a; 2012b].

To the best of authors' knowledge, experimental and numerical investigations of the incremental forming process has not been reported on explosive-welded Al/Cu bimetals so far. Therefore, in the current research, the incremental forming of a truncated pyramid is studied in Al/Cu bimetals. After validating the numerical results by the experiments, the process parameters, such as pyramid angles, tool radius, sheet thickness, vertical pitch, and process strategies, were investigated.

2. Materials and method

In the current research, a parallel arrangement was used for the experimental group of explosive-welded aluminum (Al-1050) and copper (C-10100). Chemical composition and some of the mechanical properties of these materials are given in Table 1.

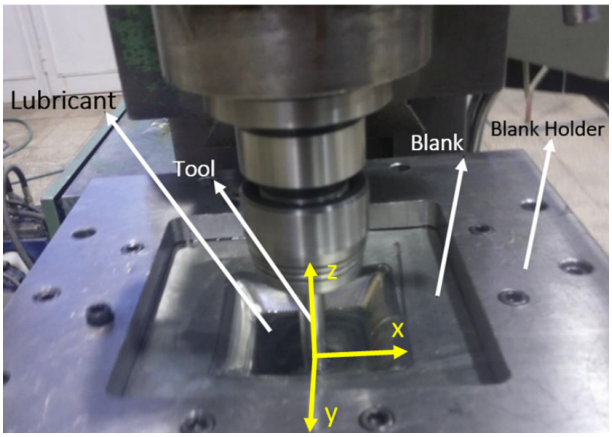

Figure 1. Incremental forming components.

A blank holder, backing plates, forming tools, and a CNC milling machine were utilized in this study. The experiments were carried out on a 3-axes CNC machine. A cylindrical punch, with a hemispherical head, was used as the tool (one-point incremental forming). The tool diameters were 10 mm and 16 mm and were made of steel Mo40 in this study. The truncated pyramids with dimensions of 72 mm × 72 mm with a 60° angle were formed in order to find the maximum depth equal to 40 mm. According to the designed equipment, square sheets (135 mm × 135 mm × 1.2 mm), were utilized during tests. The thicknesses of explosive-welded Al/Cu bimetals in the Al and Cu sheets were 0.8 mm and 0.4 mm, respectively. Figure 1 presents the used experimental setup in this study. In addition, sheet arrangement was not considered as a process parameter so a specific side of the sheet is selected for all experiments, however in future work this parameter can be studied as well. In the present study, the aluminum side of the bimetal is always in contact with the forming tool and deformation starts from that side.

In order to simulate the drawing process by finite element analysis, some of the parameters have been measured in different types of tests. In order to obtain the stress-strain curves of the used bimetals, the uniaxial tensile test performed based on ASTM-E8M standard. The tensile test was performed with a constant speed of 5 mm/min. Figure 2 illustrates the stress-strain curves of bimetal. The yield and tensile strength were 170.8 MPa and 187.2 MPa, respectively. The Coulomb friction coefficient between the tool and the sheet was equal to 0.1–0.3. These values were obtained by the experiments tests using the dynamometer forces

$$\mu = \frac{|F_h|}{|F_v|} = \frac{\sqrt{F_x^2 + F_y^2}}{F_z}, \tag{1}$$

where F_h, F_v, F_y, F_z are the horizontal force, vertical force (along forming tool axis), reaction force along x direction, reaction force along y direction, and reaction force along z direction, respectively (see Figure 1).

The spiral tool path is used to obtain the suitable strain distribution, (see Figure 3).

Lubricant was also used during the forming process to keep the temperature down at the proposed speed and stop galling as well as reducing the friction between the part and the tool. After fastening the

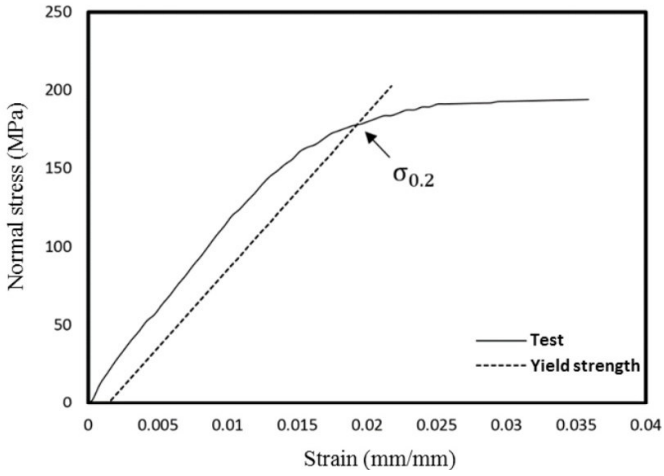

Figure 2. Stress-strain curves of explosive-welded Al/Cu bimetal before the process.

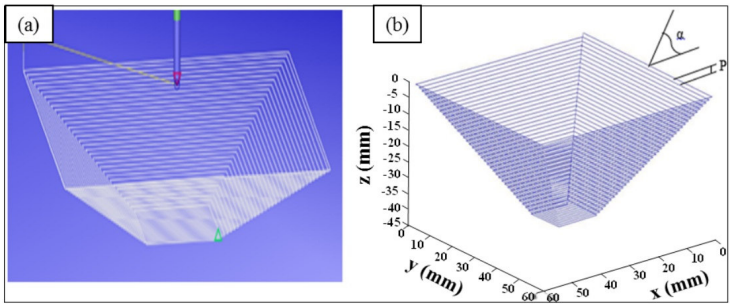

Figure 3. Schematic showing the tool path: (a) CAM software, (b) generated in the math software.

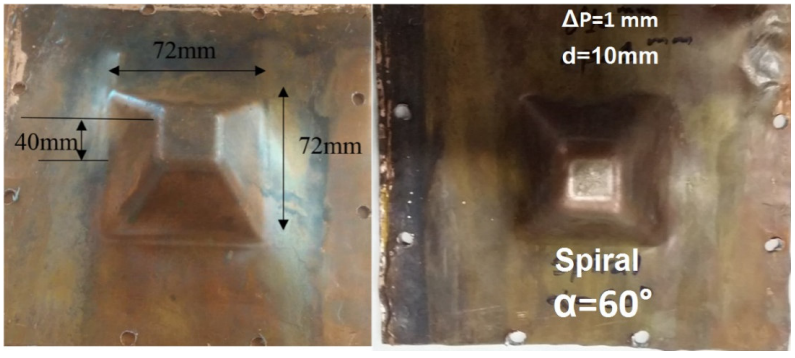

Figure 4. The formed truncated pyramid with wall angle 60°, vertical pitch 1 mm and tool diameter of: (a) 16 mm and (b) 10 mm.

blank and starting the CNC machine, the tool pushes the blank down, according to the predefined spiral path, until it reaches the maximum depth of 40 mm (see Figure 4).

tool diameters (d)	10 mm, 16 mm
vertical pitch (p)	1 mm
initial Thickness (t)	1.2 mm, 1.5 mm, 1.8 mm
rotation speed	600 rpm
height (H)	40 mm
major base	72 mm
wall angle (α)	55°, 60°, 65°
feed rate for horizontal direction (f_h)	1000 mm/min
feed rate for vertical direction (f_v)	500 mm/min

Table 2. The process parameters and geometry.

A dynamometer was used including KISTLER-9257B with six-component force sensor and a KISTLER-5017A 8 channel charge amplifier. The measuring system also includes data acquisition cards and a PC. The sampling rate of force measurement was 50 Hz. Finally, the used process parameters are summarized in Table 2. Moreover, there were two hemisphere tools with diameters (denoted by d) 10 mm and 16 mm. The wall angle of the truncated pyramid is denoted by α, which varies between 55° to 65°. Initial thickness (t) refers to thickness of the sheets before the forming process. Vertical pitch (p) is the amount of each step along z direction.

3. FEM procedures

The simulation process was performed using Abaqus finite element software. Both the explicit and implicit method can be used for this solution. However, the implicit solution showed better conformance with experimental results. On the other hand, much more computation time is required even for forming a simple shape and short tool path in implicit mode. Jeswiet et al. [2005] showed that the explicit solution needs less analysis time, and since it produces acceptable results and is suitable for generating the applicable curves, hundreds of solutions were required. In the current study, the explicit solver is employed during the entirety of FE analysis. The tool and blank holder were considered to be rigid (analytical rigid). The behavior of the stress-strain of explosive-welded Al/Cu bimetal is modeled in Figure 2. The holder was fixed and the tool can only move along the three main axes, i.e., x, y, and z along the programmed spiral path. The spiral tool path is defined in the developed VDISP subroutine; the feed rates for the horizontal direction and vertical direction were respectively 1000 mm/min and 500 mm/min.

4. Results and discussion

In this section, the numerical model and experimental results for the forming force and thickness distribution are compared. Then, the process parameters and machining strategies are numerically analyzed.

4.1. ***Validation the numerical model.*** The mesh sensitivity analysis was performed to obtain the best mesh size (see Figure 5). As it can be seen, the vertical force is relatively constant after the element number is greater than 2000.

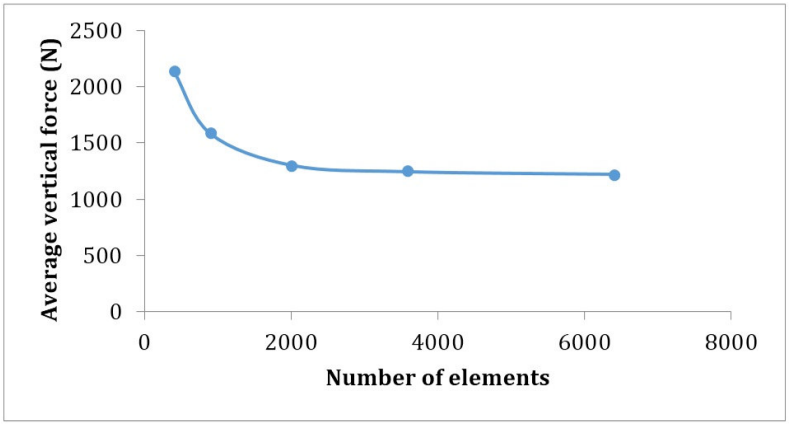

Figure 5. Mesh sensitivity analysis.

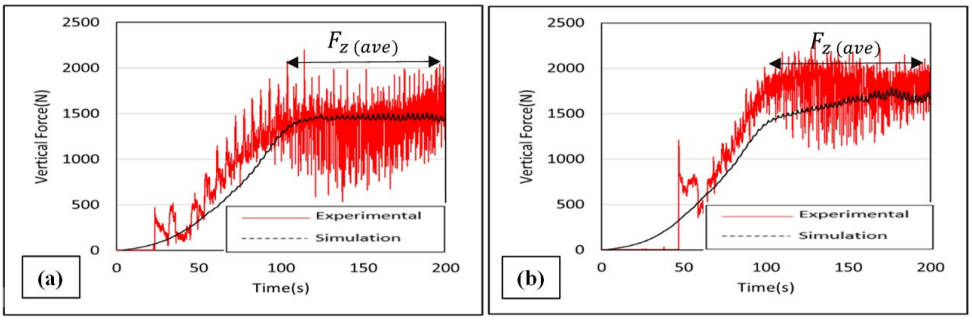

Figure 6. Experimental and numerical results of vertical force for tool diameter of: (a) 10 mm and (b) 16 mm.

To validate the numerical results, the results of the vertical forces for two diameters of forming tool are presented in Figure 6. The constant parameters are these: bimetal thickness of 1.2 mm, vertical pitch of 1 mm, and pyramid angle of 60°.

The average vertical force is useful for comparison purposes: it is calculated by taking the average of all measured or calculated F_z at a steady region (see Figure 6). The average vertical force ($F_{z(\text{ave})}$) for a tool diameter of 10 mm for the numerical and experimental results are 1464 N and 1357 N, respectively. Moreover, the average vertical forces are 1636 N and 1730 N for a tool diameter of 16 mm using FEM and experimental approaches, respectively. The maximum error for the two presented cases is equal to 9.6%, which demonstrates the suitability of FEM for predicting the forming force.

The experimental, theoretical, and numerical formed profiles are presented in Figure 7. The deviation is due to the difference of the resultant profile or thickness from the reference state, and it can be named as an error. Moreover, the reference or theoretical state refers to a desired position where a component is expected to find the plate. Thus, the maximum deviation of the experimental and FEM results is less than 10%. Also, the thickness distribution of the formed bimetal is presented in Figure 8. The experimental profile has been measured by the help of a coordinate measuring machine (CMM).

The error between FEM and experimental results is lower than 6% in the thickness distribution.

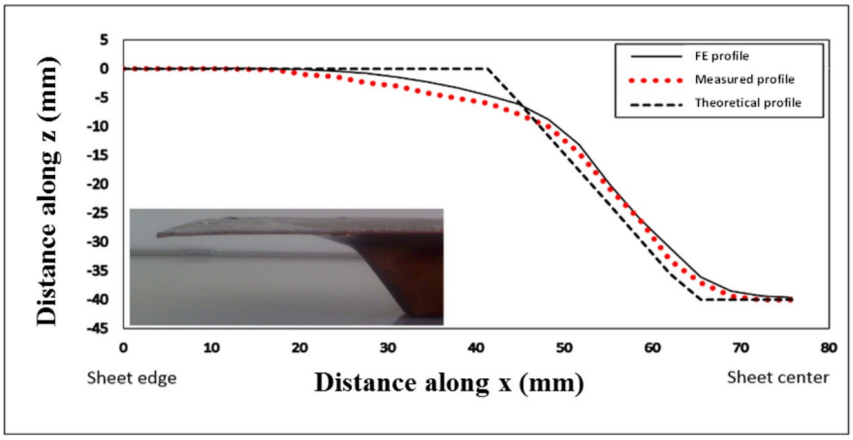

Figure 7. Comparison of the experimental, theoretical, and numerical profile for $d = 16\,\text{mm}$, $p = 1\,\text{mm}$, $\alpha = 60°$.

4.2. ***FEM results of process parameters.*** After validating the finite element model and in order to investigate the effects of process parameters, the numerical results are presented in this section. The depth of the formed pyramids is equal to 40 mm. The starting base side of pyramids is 72 mm and the minor size of the samples depends on the value of wall inclination angle α.

Two tools with 10 mm and 16 mm diameters were used in the FEM analysis. The wall angle of the truncated pyramid was 60° and vertical pitches of 0.25 mm and 1 mm were compared together. The FEM results of vertical force and thickness distribution are presented in Figures 9 and 10.

As it can be observed in Figure 9(a), vertical forces are at a maximum for a vertical pitch of 0.25 mm when tool diameter is 16 mm, and it can be inferred that the bigger tool requires greater force in smaller pitch size. Moreover, Figure 9(b) indicates that the maximum vertical force for the vertical pitch of 1 mm is greater compared to the 0.25 mm one and it is about 2 kN. This means that a greater tool diameter and vertical pitch provide greater a reaction force. It also can be seen in Figure 10 that the thicker plate can be obtained by incremental forming using a forming tool with 10 mm diameter. This means that the lower tool diameter creates thicker parts, which is a good piece of knowledge to improve part thickness during SPIF. The two step down are presented in Figure 11.

The effect of vertical pitch on the vertical force is presented in Figure 12. It can be seen that the vertical force is greater for a tool diameter of 10 mm and a vertical pitch of 1 mm. Therefore, it is inferred that the greater tool diameter and smaller vertical pitch provides lower vertical forming force in SPIF process for the Al/Cu bimetal.

The thickness distribution for each case is seen in Figure 13. Results show that by increasing the vertical pitch, the forming force increases and the thickness distribution is more uniform, which means that a thicker SPIF part can be achieved.

The effect of the initial thickness of the bimetal on the forming force is presented in Figure 14. As could be expected, the forming force is increased by increasing the initial thickness of the bimetal. The effect of wall angles on the vertical force is presented in Figure 15. The process has been modeled at 55°, 60°, and 65° wall angles.

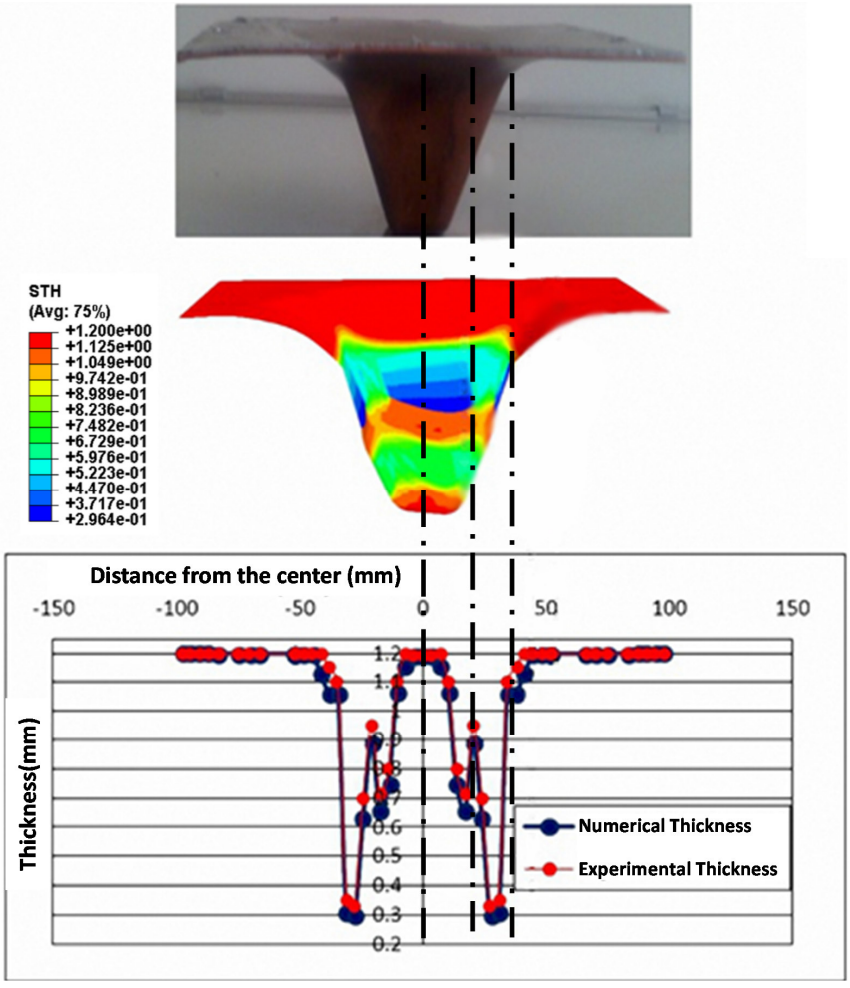

Figure 8. Comparison of the experiment and numerical thickness for $d = 16$ mm, $p = 1$ mm, $\alpha = 60°$.

4.3. ***Effect of process strategies on dimensional accuracy and thickness distribution.*** The geometrical accuracy of the final products is an important issue for industrial products, especially for SPIF products. However, the nature of the SPIF process makes it difficult to achieve a high level of geometrical accuracy. Besides, different process strategies may help to achieve a high level of geometrical accuracy.

In this section, the effect of attaching a backing plate and a kinematic support as process strategies on the geometrical accuracy are investigated by FEM. The process parameters of 16 mm tool diameter, 60° wall angle, vertical pitch of 1 mm, and bimetal thickness 1.2 mm are considered for the all strategies. The process strategies are as the following:

(1) The SPIF with a backing plate.

(2) The SPIF without a backing plate

(3) A counter tool is used in addition to the backing plate (see Figure 16).

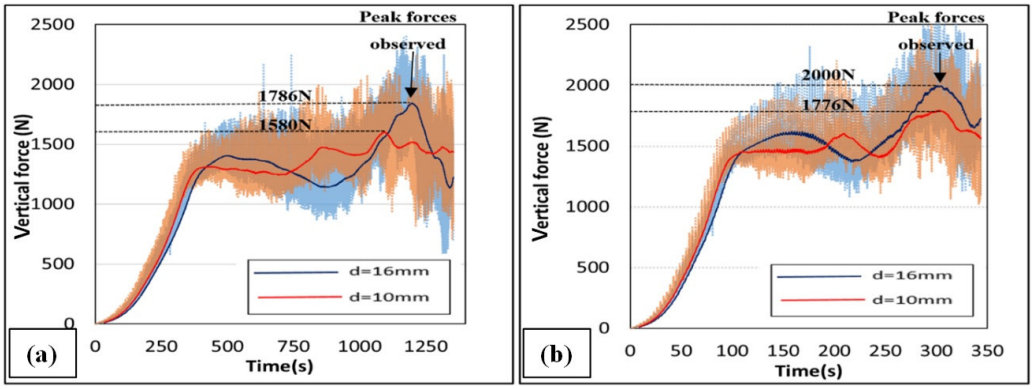

Figure 9. Vertical forces including their mean values using FEM for two tool diameters and vertical pitches of: (a) 0.25 mm (b) 1 mm.

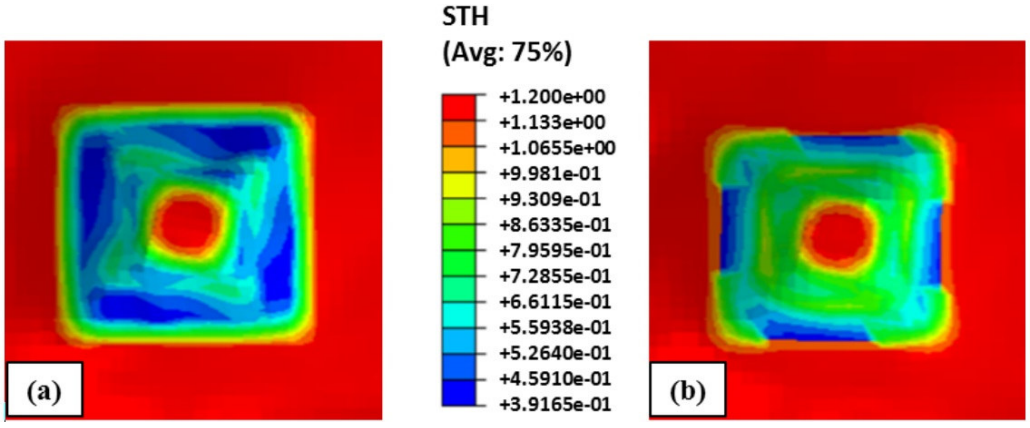

Figure 10. Thickness distributions in the vertical pitch 1 mm for tool diameter of: (a) 10 mm and (b) 16 mm.

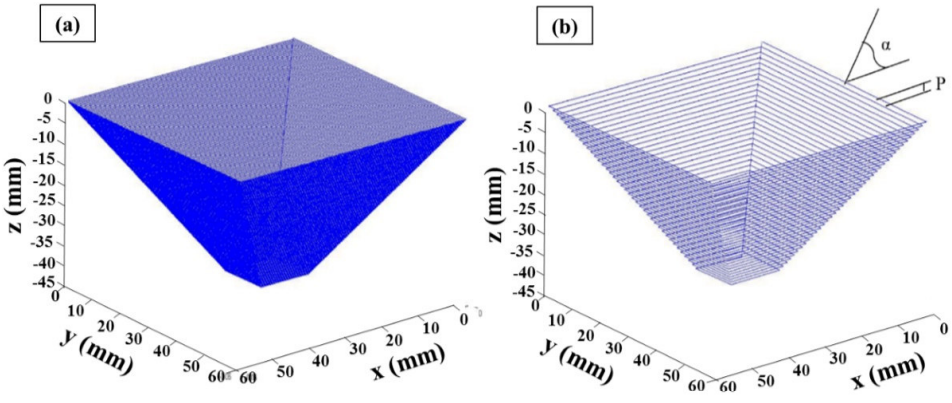

Figure 11. Tool path with step down: (a) 0.25 mm; (b) 1 mm.

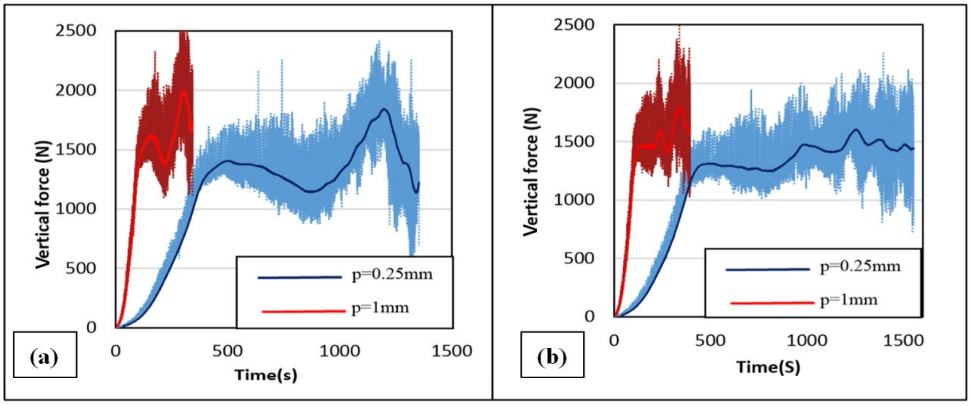

Figure 12. The effect of vertical pitches on the average vertical force in tool diameters: (a) 10 mm; (b) 16 mm.

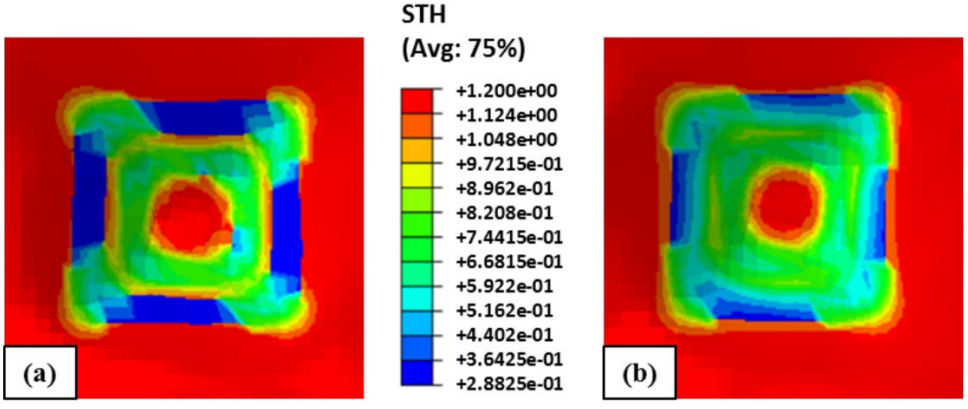

Figure 13. Thickness distributions for tool diameter 16 mm for vertical pitches: (a) 0.25 mm (b) 1 mm.

In the third strategy, a supporting counter tool is used in spite of the backing plate. The forming tool and the counter tool act in a synchronized motion and gradually form the blank sheet into the desired shape, as shown in Figure 16. The counter tool has the same geometry and dimension as the forming tool. It is modeled as a rigid body and its boundary condition is defined so that it moves in a synchronized motion with the forming tool in the XY plane and is always in contact with the bottom surface of the sheet. Surface to surface contact between the counter tool and the bottom surface of the sheet is defined and Coulomb friction is set with a friction coefficient of 0.06.

Geometrical accuracy can be represented with geometrical errors as long as the errors are at a minimum the accuracy is at a maximum. The geometrical errors are evaluated as the distance between the theoretical and FEM profiles [Micari et al. 2007]. According to this definition, two measures e_b and e_s are used to represent the geometry deviation (see Figure 17). The deviation at the upper edge is given by e_b, which represents the geometrical error resulting from the sheet bending. The deviation at the minor base is shown by e_s, which represents the sheet lifting from spring back.

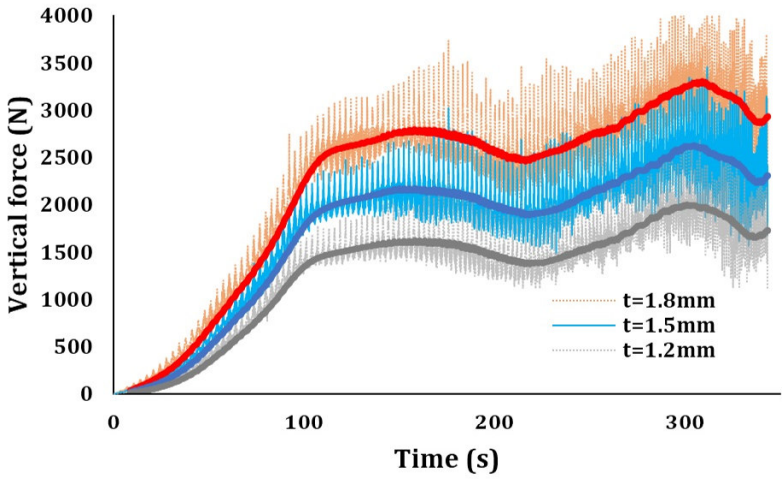

Figure 14. The effect of bimetal thickness on the vertical force curve ($d = 16\,\text{mm}$, $p = 1\,\text{mm}$, $\alpha = 60°$).

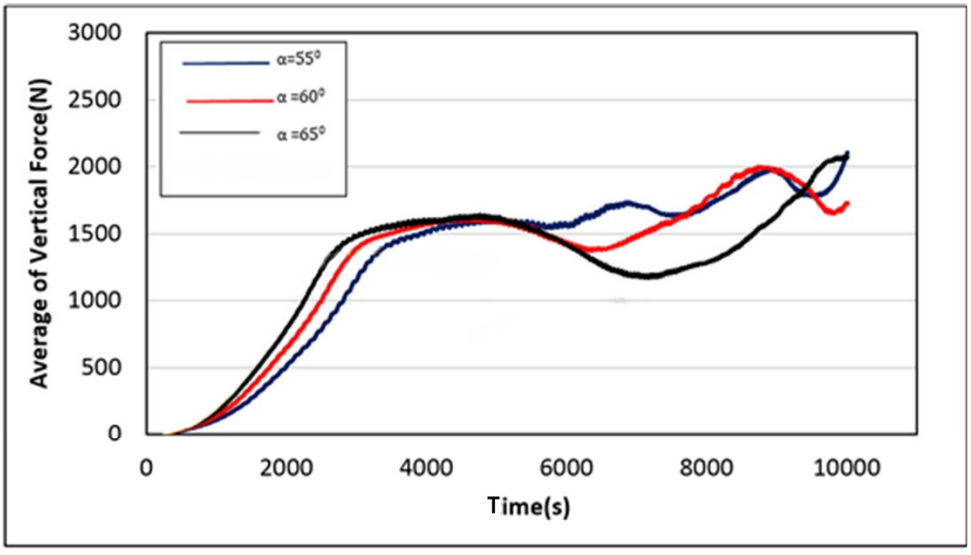

Figure 15. The effect of wall angles on the average vertical force; tool diameter (d) = 16 mm, vertical pitch (p) = 1 mm, initial thickness (t) = 1.2 mm.

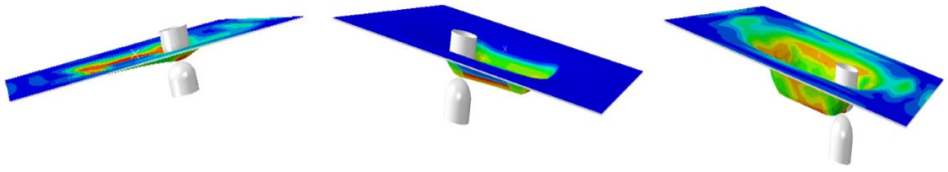

Figure 16. The configuration of the FE model of strategy 3.

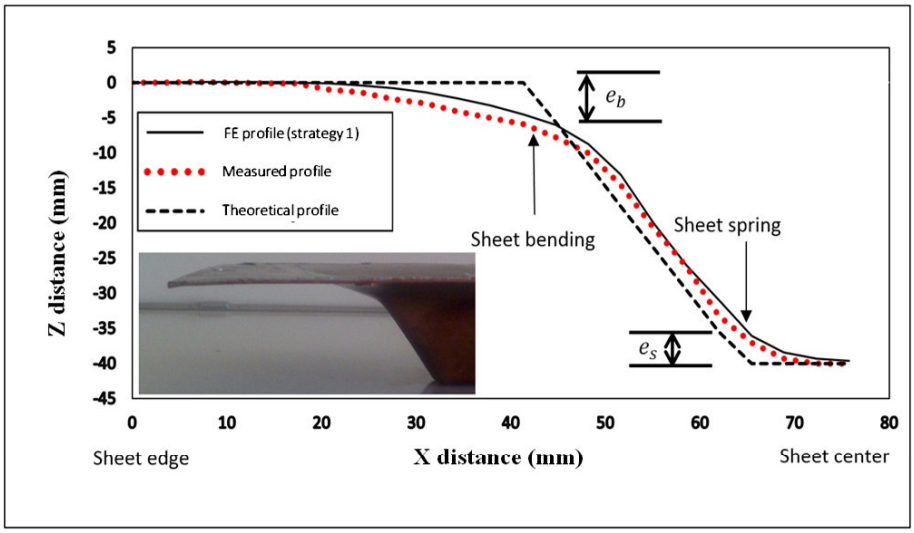

Figure 17. Deformed profile of the 60° truncated pyramid.

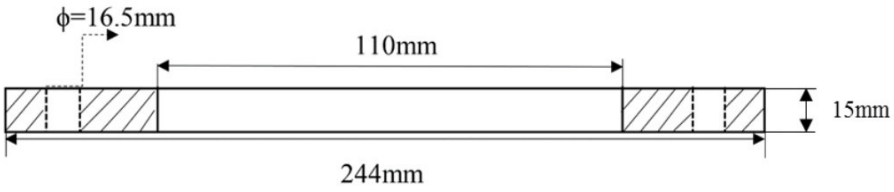

Figure 18. Dimensions (mm) and geometries of the designed backing plate.

Figure 18 shows the geometry and dimensions of the backing plate used for the truncated pyramid. All fixture components including backing plate except screws were made from CK45 steel.

The obtained values of e_b and e_s for Strategy (1) are 4.58 mm and 3.91 mm, respectively. The thickness distribution along the central plane of the deformed sheet is shown in Figure 8. It can be seen that sheet thinning increases as the truncated pyramid depth increases. At a certain point near the pyramid base, less thinning is apparent and the thickness is very close to its original value. This would be expected in Strategy (1). The reason for less thinning near the pyramid base might be that the actual slope angle is smaller than its target value due to the bending effect around the pyramid base. There is a good agreement between the FEM and the measured thickness variation.

Elastic spring back will occur locally during deformation and globally after the forming process. The resulting spring back from postprocessing, such as trimming, has not been considered in the present work. The local spring back could be reduced by using static dies as well [Franzen et al. 2008].

The elimination of the backing plate in second strategy reduces the supporting structure and maximizes this distance. Strategy (2) can illustrate the effect of the backing plate on geometrical deviations, in which deviation is the sheet bending at the major base. Figure 19 shows a comparison between Strategy (1) and (2) to indicate the impact of the backing plate on the final profile. It can be seen that the profile deviation

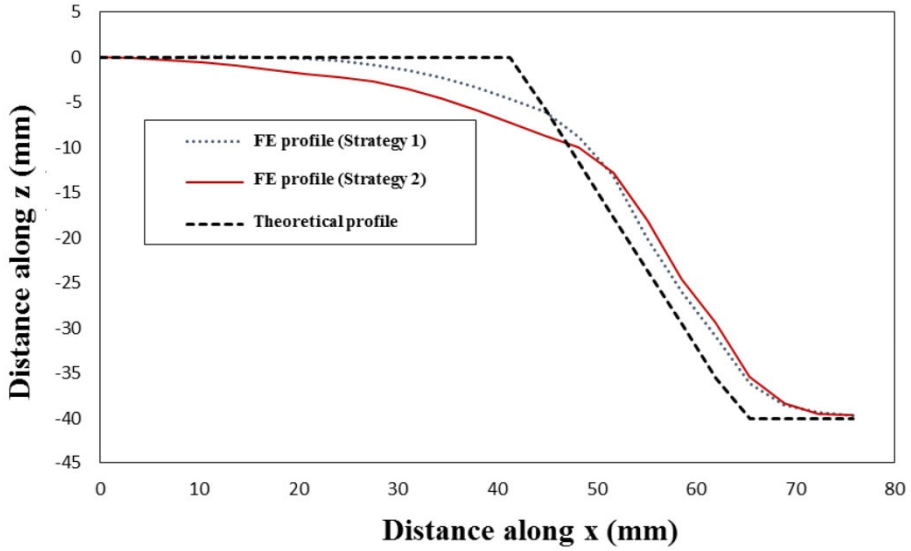

Figure 19. Effect of the backing plate on the final profile.

for Strategy (1) is less than for Strategy (2). This means Strategy (1) provides higher geometrical accuracy compared to Strategy (2).

In Strategy (3), both the counter tool and the backing plate have been used, as suggested in [Franzen et al. 2008]. In this strategy, the forming tool and the counter tool move simultaneously and incrementally form the blank sheet into the desired shape, as shown in the Figure 16. The supporting tool has the same dimensions and shape as the forming tool. Surface to surface contact was considered between the tools and sheet surfaces using Coulomb friction with a friction coefficient of 0.2.

In order to illustrate the effect of the counter tool on the geometrical errors, a comparison was performed between Strategy (1) and (3); see Figure 20. At the major base and sheet center of the truncated pyramid, there is difference between Strategy (1) and (3), which means that the kinematic supporting tool affects either the sheet bending or the spring back effect. Also it can be seen that Strategy (3) provides better geometrical accuracy compared to Strategy (1).

A significant increase in the sheet bending around the major base is obtained by Strategy (2). The backing plate can increase the sheet rigidity by introducing extra support located at the deformation zone. The results show that e_b, increases from 4.58 mm to 7.28 mm, while e_s is found to be 4.63 mm. This suggests that the backing plate can only reduce the deviation resulting from the bending effect and it cannot affect on the deviation resulting from the sheet spring back. In Strategy (3), along the pyramid wall until the minor base, there is a significant reduction in sheet spring back as a result of adding a new kinematic tool. The results show that only e_s reduces from 3.91 mm to 2.53 mm by Strategy (3). The kinematic supporting tool provides a larger localization of the deformation around the forming tool head and it also reduces the local spring back. In addition, the pyramid wall created from Strategy (3) is close to the theoretical profile and the sheet lifting of the minor base of the truncated pyramid is less than that in Strategy (2)2. Figure 21 shows the typical values for the different deviation measurements gained from the three strategies. The best geometrical accuracy is obtained using the Strategy (3), which includes adding a backing plate and a counter tool.

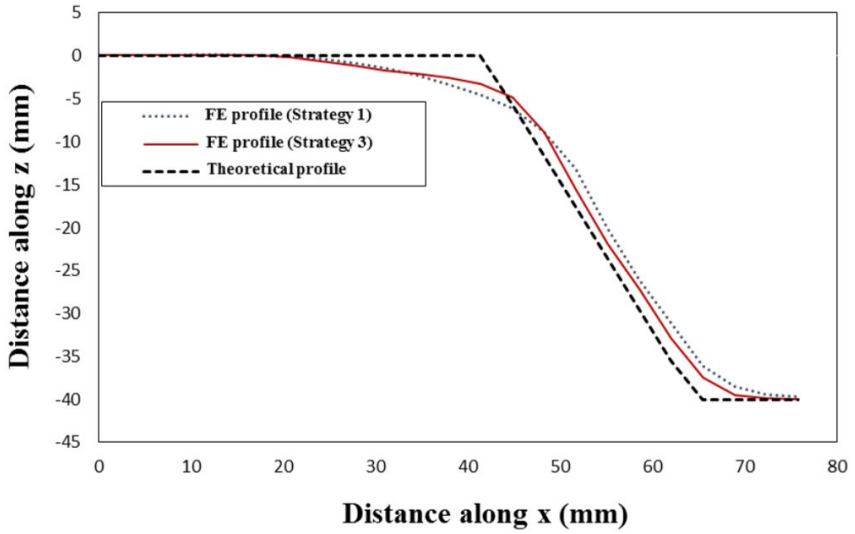

Figure 20. Effect of the kinematic supporting tool on the final profile.

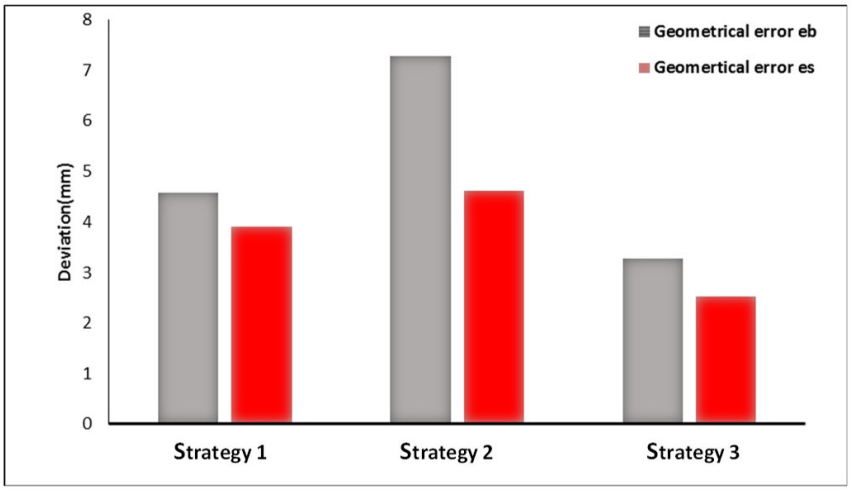

Figure 21. Summary of deviations obtained from the three strategies.

Figure 22 shows a comparison among the strategies for the vertical displacement at the end of the process, when the forming tool reaches the base of the pyramid. Figure 22(a) shows vertical displacement distribution for Strategy (1). It can be seen that there is no wrinkling for Strategy (3) (see Figure 22(c)). Moreover, SPIF with Strategy (2) produces higher wrinkling compared to other strategies.

5. Conclusion

In this study, the effects of process parameters of single point incremental forming of explosive-welded Al/Cu bimetal sheets have been numerically and experimentally investigated. The results of a truncated

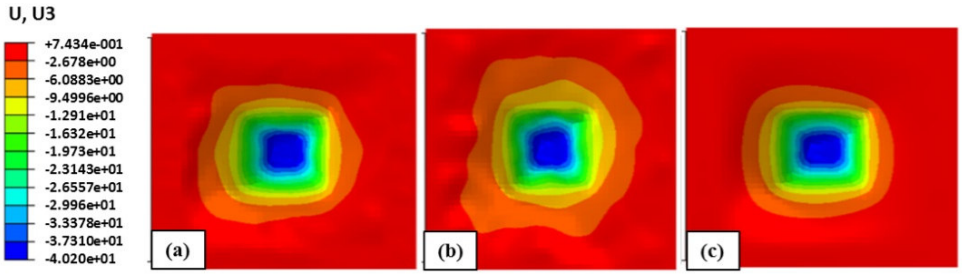

Figure 22. Contour plots for vertical distance distribution in (a) Strategy (1) (b) Strategy (2) (c) Strategy (3) of a truncated pyramidal geometry.

pyramid with depth 40 mm have been obtained for various tool diameters, vertical pitches, sheet thicknesses, pyramid wall angles, and process strategies to generate applied curves for the effective parameters on forming force, thickness distribution, and dimensional accuracy. The results are summarized in the following:

- The vertical force decreases by decreasing the tool diameter from 16 mm to 10 mm.
- The forming force increases by increasing the vertical pitch from 0.25 mm to 1 mm.
- At the beginning of SPIF process (i.e., transient region), the vertical force increases by increasing the wall angle from 55° to 65° and it gradually acts in different way: by increasing the slope angle, the force decreases (on average) when the forming tool enters the steady region.

In the second part of the work, a number of strategies were compared. In this investigation, three FE simulations of the considered process were performed for the truncated pyramidal models. For the forming of a truncated pyramid, the effects of different process strategies (i.e., the elimination of a backing plate and the addition of a kinematic supporting tool) on the geometrical accuracy were investigated. This study demonstrated the following:

- The elimination of a backing plate caused the increasing in the region closer to the major base.
- Existence a counter tool declined the deviation at the major base.
- In the strategy 3 with using a backing plate and counter tool reduced the deviation in product profile.
- In the study of a truncated pyramid, the geometrical deviations could be reduced from 7.28 mm and 4.63 mm to 3.21 mm and 2.53 mm at the major base and minor base respectively.

Acknowledgements

The authors are grateful to University of Kashan for supporting this work by giving research grant No. 682580/6.

References

[Akbari Mousavi and Sartangi 2008] S. A. A. Akbari Mousavi and P. F. Sartangi, “Effect of post-weld heat treatment on the interface microstructure of explosively welded titanium-stainless steel composite”, *Mater. Sci. Eng. A* **494**:1-2 (2008), 329–336.

[Ambrogio et al. 2004] G. Ambrogio, I. Costantino, L. De Napoli, L. Filice, L. Fratini, and M. Muzzupappa, "Influence of some relevant process parameters on the dimensional accuracy in incremental forming: a numerical and experimental investigation", *J. Mater. Process. Technol.* **153-154** (2004), 501–507.

[Arfa et al. 2013] H. Arfa, R. Bahloul, and H. BelHadjSalah, "Finite element modelling and experimental investigation of single point incremental forming process of aluminum sheets: influence of process parameters on punch force monitoring and on mechanical and geometrical quality of parts", *Int. J. Mater. Form.* **6**:4 (2013), 483–510.

[Asemabadi et al. 2012] M. Asemabadi, M. Sedighi, and M. Honarpisheh, "Investigation of cold rolling influence on the mechanical properties of explosive-welded Al/Cu bimetal", *Mater. Sci. Eng. A* **558** (2012), 144–149.

[Ashani and Bagheri 2009] J. Z. Ashani and S. M. Bagheri, "Explosive scarf welding of aluminum to copper plates and their interface properties", *Materialwiss. Werkst.* **40**:9 (2009), 690–698.

[Bao et al. 2015] W. Bao, X. Chu, S. Lin, and J. Gao, "Experimental investigation on formability and microstructure of AZ31B alloy in electropulse-assisted incremental forming", *Mater. Des.* **87** (2015), 632–639.

[Capece Minutolo et al. 2007] F. Capece Minutolo, M. Durante, A. Formisano, and A. Langella, "Evaluation of the maximum slope angle of simple geometries carried out by incremental forming process", *J. Mater. Process. Technol.* **194**:1-3 (2007), 145–150.

[Centeno et al. 2014] G. Centeno, I. Bagudanch, A. J. Martínez-Donaire, M. L. García-Romeu, and C. Vallellano, "Critical analysis of necking and fracture limit strains and forming forces in single-point incremental forming", *Mater. Des.* **63** (2014), 20–29.

[Cui et al. 2013] Z. Cui, Z. C. Xia, F. Ren, V. Kiridena, and L. Gao, "Modeling and validation of deformation process for incremental sheet forming", *J. Manuf. Process.* **15**:2 (2013), 236–241.

[Franzen et al. 2008] V. Franzen, L. Kwiatkowski, G. Sebastiani, R. Shankar, A. E. Tekkaya, and M. Kleiner, "Dyna-die: towards full kinematic incremental forming", *Int. J. Mater. Form.* **1**:1 (2008), 1163–1166.

[Gulenc 2008] B. Gulenc, "Investigation of interface properties and weldability of aluminum and copper plates by explosive welding method", *Mater. Des.* **29**:1 (2008), 275–278.

[Hirt et al. 2004] G. Hirt, J. Ames, M. Bambach, and R. Kopp, "Forming strategies and process modelling for CNC incremental sheet forming", *CIRP Ann.* **53**:1 (2004), 203–206.

[Honarpisheh et al. 2012] M. Honarpisheh, M. Asemabadi, and M. Sedighi, "Investigation of annealing treatment on the interfacial properties of explosive-welded Al/Cu/Al multilayer", *Mater. Des.* **37** (2012), 122–127.

[Honarpisheh et al. 2016a] M. Honarpisheh, M. J. Abdolhoseini, and S. Amini, "Experimental and numerical investigation of the hot incremental forming of Ti-6Al-4V sheet using electrical current", *Int. J. Adv. Manuf. Technol.* **83**:9-12 (2016), 2027–2037.

[Honarpisheh et al. 2016b] M. Honarpisheh, J. Niksokhan, and F. Nazari, "Investigation of the effects of cold rolling on the mechanical properties of explosively-welded Al/St/Al multilayer sheet", *Metall. Res. Technol.* **113**:1 (2016), art. id. 105.

[Jeswiet et al. 2005] J. Jeswiet, F. Micari, G. Hirt, A. Bramley, J. Duflou, and J. Allwood, "Asymmetric single point incremental forming of sheet metal", *CIRP Ann.* **54**:2 (2005), 88–114.

[Manco and Ambrogio 2010] G. L. Manco and G. Ambrogio, "Influence of thickness on formability in 6082-T6", *Int. J. Mater. Form.* **3**:1 (2010), 983–986.

[Martins et al. 2008] P. A. F. Martins, N. Bay, M. Skjødt, and M. B. Silva, "Theory of single point incremental forming", *CIRP Ann.* **57**:1 (2008), 247–252.

[Micari et al. 2007] F. Micari, G. Ambrogio, and L. Filice, "Shape and dimensional accuracy in single point incremental forming: state of the art and future trends", *J. Mater. Process. Technol.* **191**:1-3 (2007), 390–395.

[Mulay et al. 2017] A. Mulay, S. Ben, S. Ismail, and A. Kocanda, "Experimental investigations into the effects of SPIF forming conditions on surface roughness and formability by design of experiments", *J. Brazil. Soc. Mech. Sci. Eng.* **39**:10 (2017), 3997–4010.

[Obikawa et al. 2009] T. Obikawa, S. Satou, and T. Hakutani, "Dieless incremental micro-forming of miniature shell objects of aluminum foils", *Int. J. Mach. Tool. Manuf.* **49**:12-13 (2009), 906–915.

[Petek et al. 2009] A. Petek, K. Kuzman, and J. Kopač, "Deformations and forces analysis of single point incremental sheet metal forming", *Arch. Mater. Sci. Eng.* **35**:2 (2009), 107–116.

[Reddy and Cao 2009] N. V. Reddy and J. Cao, "Incremental sheet metal forming: a review", review, Indian Institute of Technology Kanpur, 2009, Available at https://tinyurl.com/sheetreview.

[Sedighi and Honarpisheh 2012a] M. Sedighi and M. Honarpisheh, "Experimental study of through-depth residual stress in explosive welded Al/Cu/Al multilayer", *Mater. Des.* **37** (2012), 577–581.

[Sedighi and Honarpisheh 2012b] M. Sedighi and M. Honarpisheh, "Investigation of cold rolling influence on near surface residual stress distribution in explosive welded multilayer", *Strength Mater.* **44**:6 (2012), 693–698.

[Silva et al. 2011] M. B. Silva, P. S. Nielsen, N. Bay, and P. A. F. Martins, "Failure mechanisms in single-point incremental forming of metals", *Int. J. Adv. Manuf. Technol.* **56**:9-12 (2011), 893–903.

[Thibaud et al. 2012] S. Thibaud, R. B. Hmida, F. Richard, and P. Malécot, "A fully parametric toolbox for the simulation of single point incremental sheet forming process: numerical feasibility and experimental validation", *Simul. Model. Pract. Theory* **29** (2012), 32–43.

[Yamashita et al. 2008] M. Yamashita, M. Gotoh, and S.-Y. Atsumi, "Numerical simulation of incremental forming of sheet metal", *J. Mater. Process. Technol.* **199**:1-3 (2008), 163–172.

Received 29 Jun 2017. Revised 5 Oct 2017. Accepted 5 Nov 2017.

MOHAMMAD HONARPISHEH: honarpishe@kashanu.ac.ir
University of Kashan, Kashan, Iran

MORTEZA KEIMASI: keimasimorteza@gmail.com
University of Kashan, Kashan, Iran

IMAN ALINAGHIAN: iman.algh@gmail.com
University of Kashan, Kashan, Iran